Structural Engineering and Mechanics, *Vol. 55, No. 1 (2015) 205-228*
DOI: http://dx.doi.org/10.12989/sem.2015.55.1.205

A parametric investigation on the hysteretic behaviour of CFT column to steel beam connections

R. Esfandyary[1a], M.S. Razzaghi[2] and A. Eslami[*3]

[1]*Department of Civil Engineering, Azad University, South Tehran Branch, Tehran, Iran*
[2]*Department of Civil Engineering, Azad University, Qazvin Branch, Qazvin, Iran*
[3]*School of Civil Engineering, The University of Queensland, Australia*

(Received November 12, 2014, Revised May 15, 2015, Accepted June 9, 2015)

Abstract. The results of a numerical investigation pertaining to the hysteretic behaviour of concrete filled steel tubular (CFT) column to I-beam connections are discussed in detail. Following the verification of the numerical results against the available experimental tests, the nonlinear finite element (FE) analysis was implemented to evaluate the effects of different parameters including the column axial load, beam lateral support, shape and arrangement of stiffeners, stiffness of T-stiffeners, and the number of shear stiffeners. Pursuing this objective, an external CFT column to beam connection, tested previously, was selected as the case-study. The lateral forces on the structure were simulated, albeit approximately, using an incremental cyclic loading reversal applied at the beam tip. The results were compared in terms of hysteretic load-displacement curves, stress distributions in connection, strength, rotation, and energy dissipation capacity. It was shown that external T-stiffeners combined with internal shear stiffeners play an important role in the hysteretic performance of CFT columns to I-beam connections.

Keywords: CFT columns; steel I-beam; column to beam connections; seismic performance; hysteretic behaviour; cyclic loading

1. Introduction

Concrete filled steel tubular (CFT) columns are widely used in construction of mid- to high-rise buildings due to their great seismic performance in terms of strength and ductility. The combination of steel tube and concrete in a CFT column uses the inherent advantages of steel and concrete together. While the steel tube in a CFT column serves as a convenient formwork, it also provides lateral confinement for the cured concrete which results in improving the ductility and strength of the concrete. At the same time, the steel tube acts as longitudinal reinforcement. On the other hand, the concrete infill precludes local buckling of the CFT column wall. These advantages present CFT structures as an economic and effective structural system. Consequently, many research studies (Gardner and Goldsworthy 2005, Ghobadi *et al.* 2009, Han *et al.* 2011, Lee *et al.* 2008, Liu *et al.* 2008, Mirghaderi *et al.* 2010, Sheet *et al.* 2013, Wu *et al.* 2007, Yuan *et al.* 2014,

*Corresponding author, Ph.D. Graduate, E-mail: a.eslami@uqconnect.edu.au
[a]Graduate MSc. Student

http://www.techno-press.org/?journal=sem&subpage=8 ISSN: 1225-4568 (Print), 1598-6217 (Online)

Zhang *et al*. 2012, Zhao *et al*. 2010, Probst *et al*. 2010, Kang *et al*. 2015, Hassan *et al*. 2014) have also been conducted in the past decade on the behaviour of the concrete filled steel tubes.

In a composite CFT structure, beam-column connections are critical regions designed for inelastic response to seismic forces. The overall strength, stiffness and ductility of a structure are highly dependent upon the performance of the critical regions of beams and columns in the vicinity of beam-column connections and the joint core. Several studies can be found in the literature on the hysteretic behaviour of CFT column to steel beam connections. Schneider and Alostaz (1998) loaded six large scale connections up to failure point using the quasi-static test method. According to their experimental results, welding the girder directly to the steel tube wall can cause large deformation demands on the tube wall and, for this reason, should be avoided for moment-resisting frames constructed in active seismic regions. They also suggested some improvements such as using an embedded element or extended diaphragm to improve cyclic behaviour of the CFT connections. Elremaily and Azizinamini (2001) investigated the cyclic behaviour of the steel beam to CFT column connection using seven two-thirds scale specimens. The test specimens were designed to exhibit different failure modes including column failure, beam failure, and joint-shear failure. Their experimental outcomes were used to develop design models. In an experimental and numerical investigation, Kang *et al*. (2001) studied the effect of *T*-shaped stiffeners combined with reinforcing bar or bent plate penetrating the column on the hysteresis performance of a CFT column to beam welded connections. Their results indicated the vital role of the *T* stiffener on the hysteresis behaviour of the specimens regardless of the existence of the penetrated element. The behaviour of a welded CFT column to beam connections with external *T* stiffeners was also examined by Shin *et al*. (2004) under cyclic loading. Their experimental program comprised six full-scale specimens. The test parameters were the strength ratios of the horizontal and vertical stiffeners to the beam flange. The results showed that the specimens with a stiffener to beam flange ratio of 130% possessed a stable hysteresis behaviour and good ductility capacity without pinching. Their nonlinear FE analysis findings were also in a good agreement with their experimental observations. In a similar experimental test, Shin *et al*. (2008) investigated the seismic behaviour of seven CFT column to beam connections reinforced with horizontal and vertical *T* stiffeners with different strengths. All their specimens developed a noticeable plastic rotation. Kiamanesh *et al*. (2010) determined the effects of various stiffeners and column flange thicknesses, on energy dissipation capacity and location of plastic deformation of a welded *I* beam to CFT column connection using both experimental tests and numerical analyses. The stiffeners used comprised *T* stiffeners, column stiffeners, and top-flange and bottom-flange stiffeners. They concluded that the highest value of energy dissipation can be achieved by using both column stiffeners and top-flange stiffeners.

Based on the literature reviewed, no comprehensive parametric study has been conducted to investigate the effect of different parameters on the seismic performance of CFT column to steel beam connections. This can be due to the limited number of test specimens; something which is typically governed by the cost of experimentation. However, a nonlinear analysis approach can be used as a cost-effective tool to carry out a parametric study. Towards this, a comprehensive numerical investigation was conducted to evaluate the influence of different parameters on hysteretic behaviour of CFT column to steel I-beam connections. The finite element (FE) modelling and analysis were performed in ANSYS (2005), a commonly used program. As part of this research, Razzaghi *et al*. (2014) presented the preliminary results of some specimens pertaining on the effects of internal and external stiffener. As a complementary paper, the findings have been extended in the current study implementing more specimens. In addition, the effect of

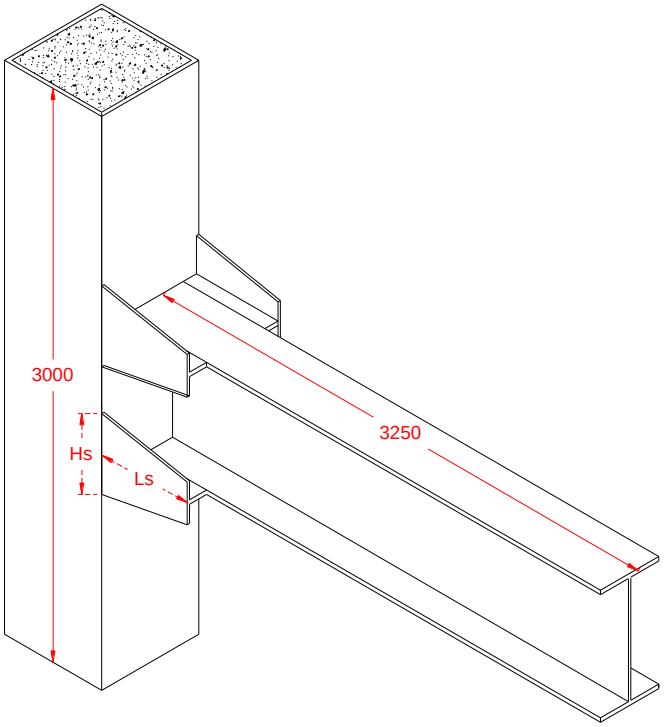

Fig. 1 Schematic illustration of the specimen TS-3

different parameters including the column axial load, beam lateral support, shape and arrangement of stiffeners, stiffness of *T*-stiffeners, and the number of shear stiffeners required are discussed in detail. The findings can improve the design of CFT structures in practical constructions.

2. FE modelling and experimental verification

Generally, the first step of every numerical study is the verification of the modelling and analysis results against the existing experimental data. Pursuing this objective, an experimental test conducted by Shin *et al*. (2004) was considered for the purpose of verification in this study. Their experimental and numerical investigation was comprised of six full-scale, CFT column to *I*-beam welded connections with *T* stiffeners. In the current study, the specimen TS-3 was modelled and the results of nonlinear FE analysis were compared with those obtained from the experimental tests. This specimen was then also adopted as the case-study for the parametric investigation of the current study. Fig. 1 shows dimension details of the specimen TS-3. The beam has a height of 588 mm, flange width of 300 mm, web thickness of 12 mm and flange thickness of 20 mm. The column was built of a square 500 mm tube with a thickness of 12 mm. Also, the height of the vertical stiffener, H_S, and the length of horizontal stiffener, l_S, were 360 mm and 440 mm, respectively. The thicknesses of the stiffeners were equal to the thickness of the connected plates.

The average compressive strength of concrete, used to fill the tube, was measured to be about 26.5 MPa. Also, the mechanical properties of steel elements determined from the tensile coupon

Table 1 Mechanical properties of the steel elements specimen TS-3 (Shin *et al.* 2004)

Element	Yield stress (MPa)	Ultimate stress (MPa)	Elongation (%)
Beam flange	306	445	24
Beam web	319	440	28
Steel Tube	271	458	26
Horizontal stiffener	369	571	26
Vertical stiffener	289	518	26

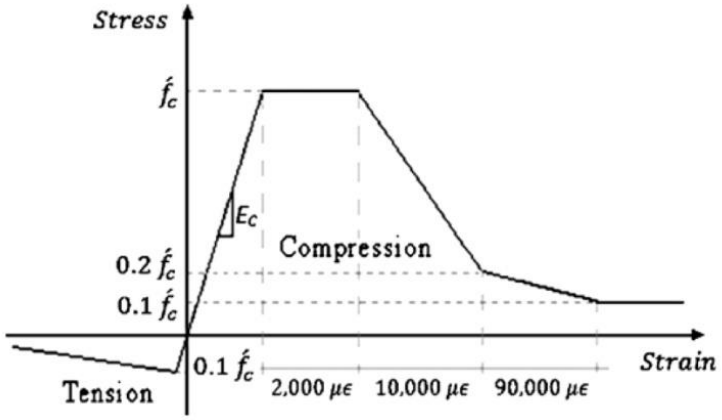

(a)

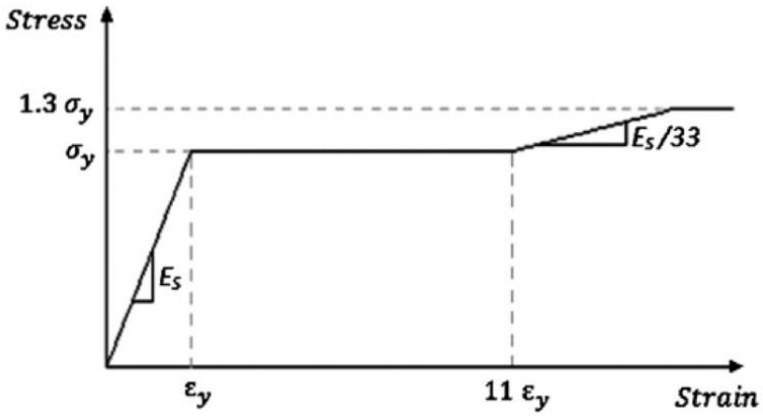

(b)

Fig. 2 Constitutive models for (a) concrete, and (b) steel

tests are summarized in Table 1. For the FE analysis of the current study, the stress-strain behaviour of the concrete and steel was simulated using the multi-linear models indicated in Fig. 2. These models were also implemented in previous numerical studies on CFT columns conducted by other researchers (Abedi *et al.* 2008).

The three-dimensional (3D) FE models of the CFT connection specimen were developed in ANSYS (2005). SOLID45, a 3D solid element, was implemented to model the steel tube, *I*-beam,

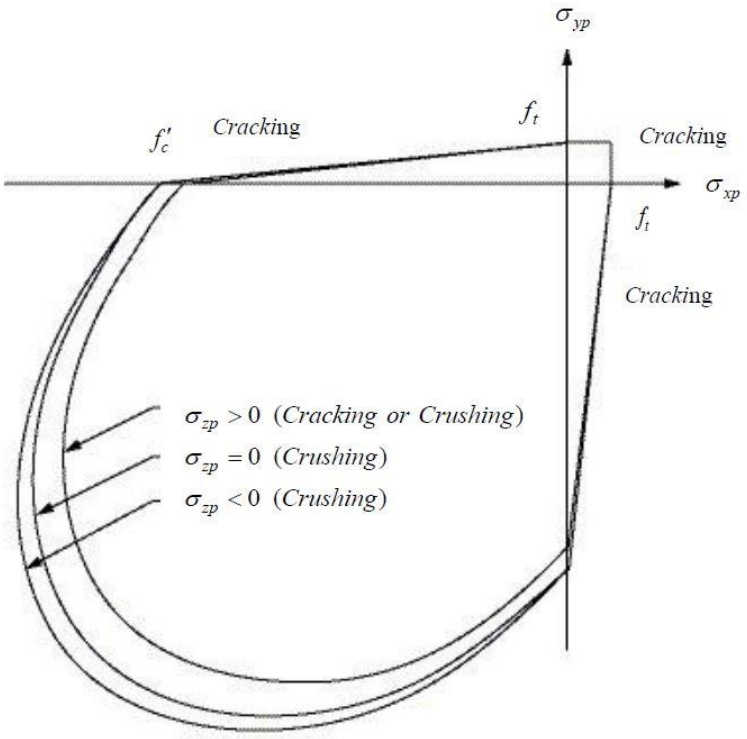

Fig. 3 3D failure surface of William-Warnke criterion

stiffeners, and shear connections. With the capability of plastic deformation, this element has eight nodes with three degree of freedom at each node (translation in the nodal *x*, *y*, and *z* directions). The material behaviour of steel was simulated using the Von-Mises yield criterion and the Kinematics hardening rule. In a welded connection, rupture of the connecting elements might be one of the failure modes. However in the current study, this type of failure was assumed to be prevented by selecting a quality and appropriate weld so that its strength is at least equal to the connected components. Thus the weld and structural steel were monolithically modelled using SOLID45. This assumption has been supported by the experimental results of specimen TS-3 where a ductile beam failure was observed without fracture of connecting elements. *A* comprehensive experimental investigation on the behaviour of weld in steel moment resisting connections and recommendations for pertinent weld type were presented by Ghobadi *et al*. (2009).

In order to model the concrete infill, the 3D eight-node concrete element, SOLID65, was employed. This solid element has three degrees of freedom at each node. It is similar to the SOLID45 with the addition of special cracking and crushing capabilities in tension and compression, respectively. It has been especially provided in ANSYS to model concrete and other quasi-brittle materials.

The William-Wranke failure criterion (Willam and Warnke 1975) was used for the fracture modelling of concrete, as shown in Fig. 3. The parameters σ_{xp}, σ_{yp}, and σ_{zp} refer to the principle stress in *x*, *y*, and *z* directions, respectively. The concrete failure mode is a function of the sign of σ_{zp}. For example, if σ_{xp} and σ_{yp} are both negative and σ_{zp} is slightly positive, cracking would be

predicted in a direction perpendicular to the σ_{zp} direction. However, if σ_{zp} is zero or slightly negative, the concrete is assumed to crush. A detailed description of the advantage and disadvantage of the William-Warnke failure criterion compared to other yield and failure models is provided in Ronagh and Baji (2014).

The William-Warnke model also uses the concept of a smeared crack model first introduced by Rashid (1968). Because, in reality concrete cracking is comprised of a system of parallel cracks continuously distributed over the concrete mass, this model represents the cracks by parallel micro-cracks distributed (smeared) over the finite elements. In this model, the cracks are considered to be an indication of a change in the material property of the element, over which the cracks are assumed to be smeared.

Amongst the important parameters which control the failure of concrete in ANSYS, are elastic modulus (E_c), concrete compressive strength (f'_c), concrete tensile strength or modulus of rupture (f_r), poisson's ratio (v), and the shear transfer coefficients for open (β_t) and closed (β_c) cracks. Both of the latter coefficients take values between 0.0 and 1.0 and represent conditions of the crack face. A value of 0 for (β_t) represents a smooth crack (complete loss of shear transfer) while a rough crack (no loss of shear transfer) is taken as 1. According to the past studies (Dalalbashi *et al*. 2012, 2013, Eslami *et al*. 2013, Kachlakev *et al*m 2001), a shear transfer coefficient, β_t, of 0.3 for open cracks provides the best estimation of experimental results. Furthermore, the shear transfer coefficient, β_c, of 0.7 is used for closed cracks, as recommended in ANSYS and past studies (Dalalbashi *et al*. 2012, 2013, Eslami *et al*. 2012, Eslami and Ronagh 2013).

The bond between the steel tube and the concrete infill was modelled using a three-dimensional point to point contact element (CONTAC52). With three translational degrees of freedom at each node, this element connects two adjacent nodes of steel wall and concrete core. It represents two surfaces which may maintain or break physical contact and may slide relative to each other. The element is capable of supporting only compression in the direction normal to the surfaces and

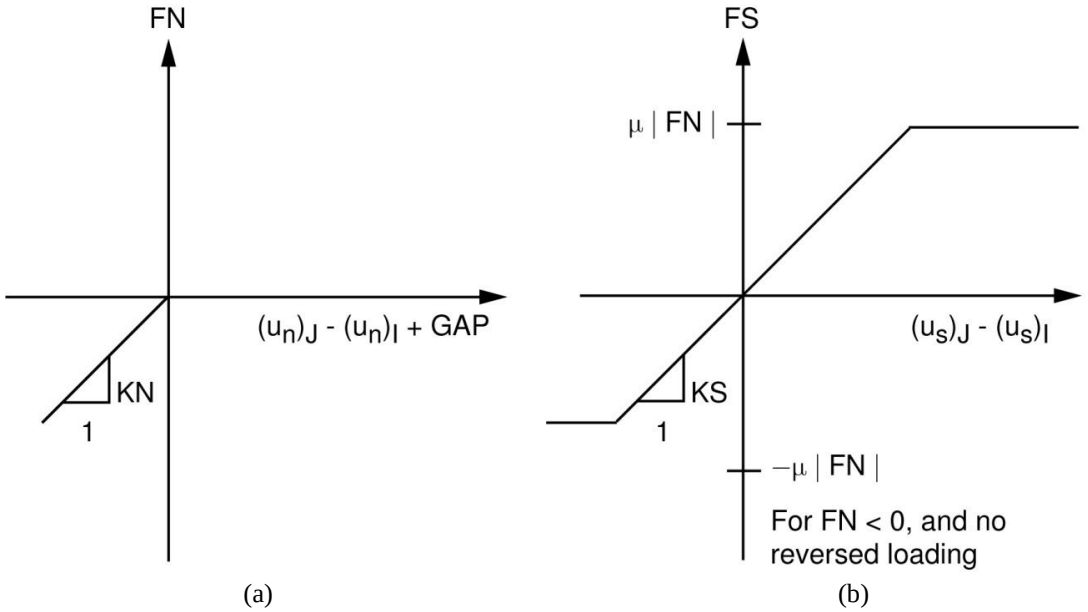

Fig. 4 CONTAC52 force-deflection relationship (ANSYS 2005)

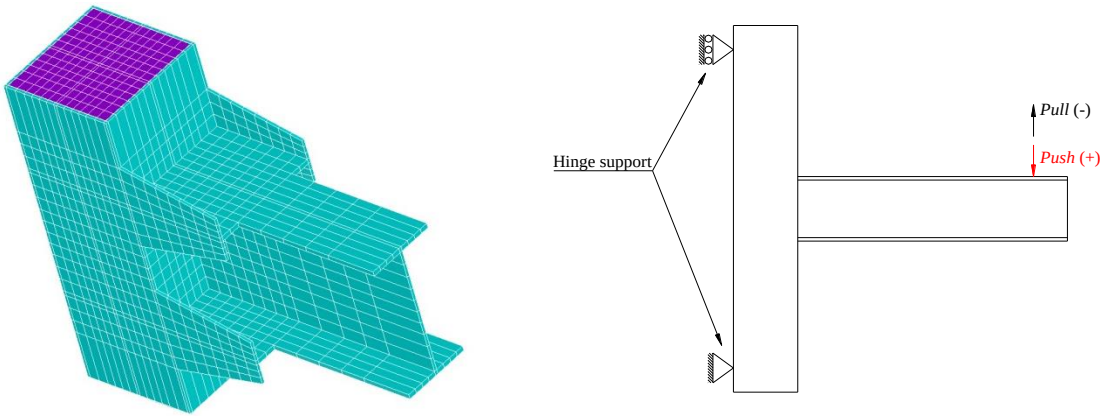

(a) (b)

Fig. 5 (a) FE model and (b) boundary conditions of specimen TS-3

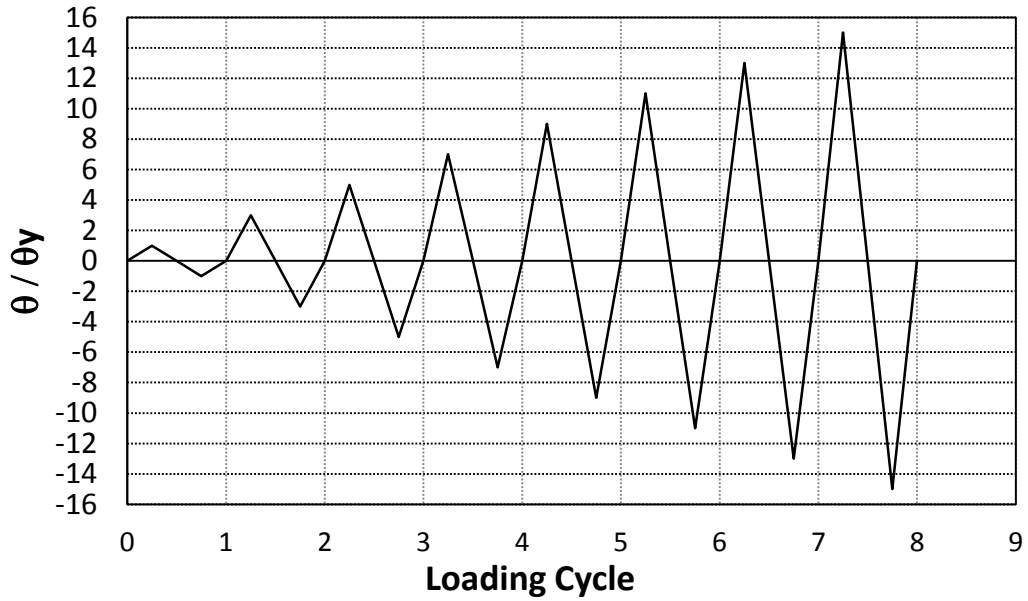

Fig. 6 Cyclic loading history

shear (Coulomb friction) in the tangential direction. The element may be initially preloaded in the normal direction or it may be given a gap specification. A specified stiffness acts in the normal and tangential directions when the gap is closed and not subject to sliding. The assumptions of CONTAC52 are friction coefficient (μ), stiffness in the normal direction (K_N), stiffness in the tangential direction (K_S), initial gap (*GAP*), and initial element status. Fig. 4 shows the force-deflection relation of this three dimensional contact element.

The FE model of specimen TS-3 developed based on the afore-mentioned assumptions is illustrated in Fig. 5(a). Also, Fig. 5(b) shows the boundary conditions used for this test specimen

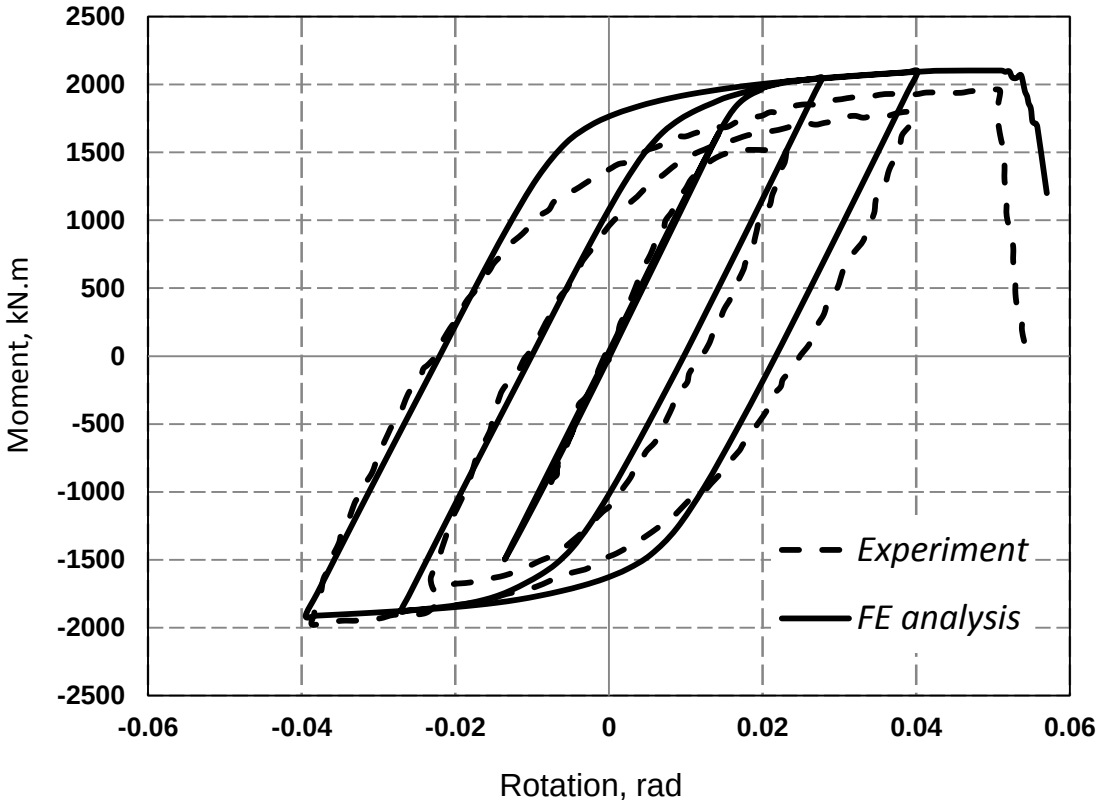

Fig. 7 Comparison of the experimental and numerical hysteretic curves

and for all other FE models developed in the current study. Similar to the experimental conditions, no lateral support was provided for the beam in the FE modelling of specimen TS-3. During the analysis, the load was applied at the beam tip using a displacement control method to avoid convergence problems and the solution was arrived using the modified Newton-Raphson method. The specimen was loaded using an incremental cyclic procedure to simulate a displacement loading reversal as shown in Fig. 6. This loading regime was applied up to failure. The total beam rotation, θ, was calculated as the tip displacement divided by the distance between the loading point and the column centreline, as reported by Shin *et al*. (2004). The yield rotation, θ_y, corresponds to the beam plastic moment. Each cycle was modelled with a load step and each load step was divided into a number of sub-steps. Due to the linear behaviour of materials at the initial step of the analysis, a lower number of sub-steps were taken. However, more load steps and sub-steps were defined subsequently to avoid convergence problems in nonlinear performance.

The beam tip load was plotted versus its corresponding rotation, as a characteristic force-displacement curve. Fig. 7 compares the hysteretic curves obtained from the nonlinear FE analysis and the experimental test. Some discrepancies between numerical and experimental curves can be due to the Bauschinger effect of steel which cannot be considered in the current version of ANSYS. This difference can be also observed in FE analysis of the same specimen performed by Shin *et al*. (2004) in ABAQUS. In general, a good agreement can be observed between the experimental and numerical results, indicating the reliability of the adopted FE analysis

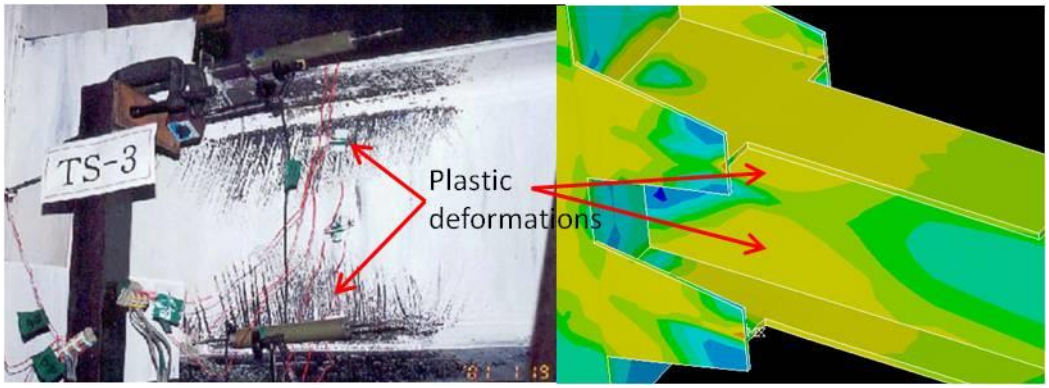

Fig. 8 Location of plastic hinge in the experimental specimen and FE model

Table 2 Mechanical properties of the steel materials in current study

Yield stress (MPa)	Ultimate stress (MPa)	Elastic modulus (GPa)	Elongation (%)
240	370	200	21

particularly in estimating the ultimate moment and rotation capacity. Also, the FE analysis was able to accurately predict the failure mode and plastic hinge location of the test specimen, as shown in Fig. 8.

3. Description of the CFT connection models

For the parametric study, the overall geometry and dimensions of beams, columns, and *T*-stiffeners in all CFT connection models were assumed to be identical to the test specimen used for verification. A similar cyclic loading history, as shown in Fig. 6, was also used during the nonlinear FE analysis. The only differences in the geometrical details were the arrangement of stiffeners and adding shear stiffeners inside the tube column. In addition, the effects of other parameters including the column axial load, beam lateral support, and different connection stiffeners in the cyclic behaviour of CFT connections were evaluated using different FE models.

In developing the FE models for parametric study, the concrete compressive strength was assumed to be about 30 MPa. Also, the mechanical properties of steel were considered to be the same for all members, and are given in Table 2.

4. Considered parameters and FE results

The variations considered in this study were column axial load, beam lateral support, shape of connection stiffeners, number of *T*-stiffeners, and number of shear stiffeners inside the tube column. In general, a total of twenty-three CFT connections were modelled in ANSYS. For the ease of discussion, the specimens were classified in five categories, based on the investigated parameters. The results are separately described in terms of hysteretic curves, stress and strain distribution, and failure modes. In the hysteretic curves, the horizontal axis is the total beam

rotation defined as tip displacement divided by the distance between the tip beam and the column centreline. The vertical axes show the connection moments normalized with respect to the beam plastic moment which was about 1388 kN.m (Shin *et al.* 2004).

To provide a better connection between concrete infill and column tube, internal shear stiffeners were also supposed to be welded at the middle of each tube side in all specimens except category *V*. In the latter, the number of shear stiffeners was considered as a variation of the study. The shear stiffener plates have a thickness of 12 mm with a width of 88 mm and a length of 3500 mm.

Although no lateral support was provided for the beam in the test specimen used for verification of the FE model, it may significantly affect the hysteretic behaviour of CFT connections. In addition, the lateral displacement of beam is usually restrained by slab in real constructions. To more scrutinise the effect of beam lateral support, the specimen in category II was analysed without any lateral support for the beam. In all other cases, the lateral displacement of top flange, bottom flange, and the web of the beam were fully restrained to consider the effect of the floor deck and to comply with the conditions of real three-dimensional constructions. It is worth mentioning that this simulates the conditions in which the beam is embedded into the concrete slab or supported by the joists of the floor deck in which mostly the top flange and web is laterally supported. The condition of the bottom flange depends on the height of the beam compared to the slab thickness or joist height. In the case that only top flange is laterally restrained by the floor deck, no lateral support should be provided for the web and bottom flange.

4.1 Category I: column axial load

The axial load on a column varies during a seismic loading depending on the lateral load carrying systems. The gravity loads on the structure also makes a considerable contribution in column axial load. In order to investigate the effect of column axial load on the hysteretic behaviour of CFT column to beam connections, nine specimens were considered with different axial loads. Table 3 provides a summary of all the specimens. The only variation was the amount of column axial load which is applied as a percentage of the ultimate compressive capacity of the column. This axial load level was selected to represent the typical range of column axial forces in practical multi-story building structures.

Table 3 Details of specimens in category I

Specimen Designation	No. of T-stiffeners	No. of Shear stiffeners	Ratio of column axial load to ultimate strength (%)
CI-1	4	4	7
CI-2	4	4	13
CI-3	4	4	17
CI-4	4	4	21
CI-5	4	4	23
CI-6	4	4	27
CI-7	4	4	29
CI-8	4	4	33
CI-9	4	4	40

The tip beam load-displacement curves and the stress distribution at the last step of loading, obtained from the nonlinear FE analysis of the specimens in category I, are shown in Fig. 9. From comparison of the results, it can be concluded that the cyclic behaviour of the CFT connection can be noticeably improved in terms of the dissipated energy and displacement capacity by increasing

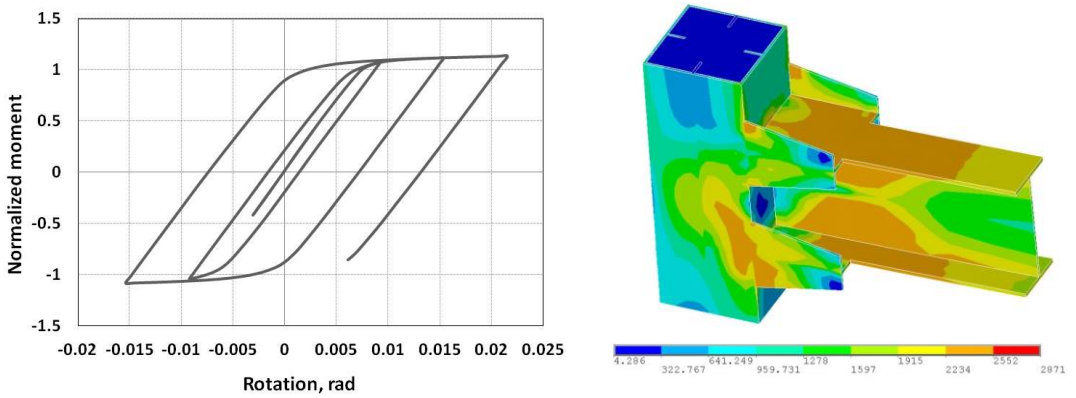

CI-1

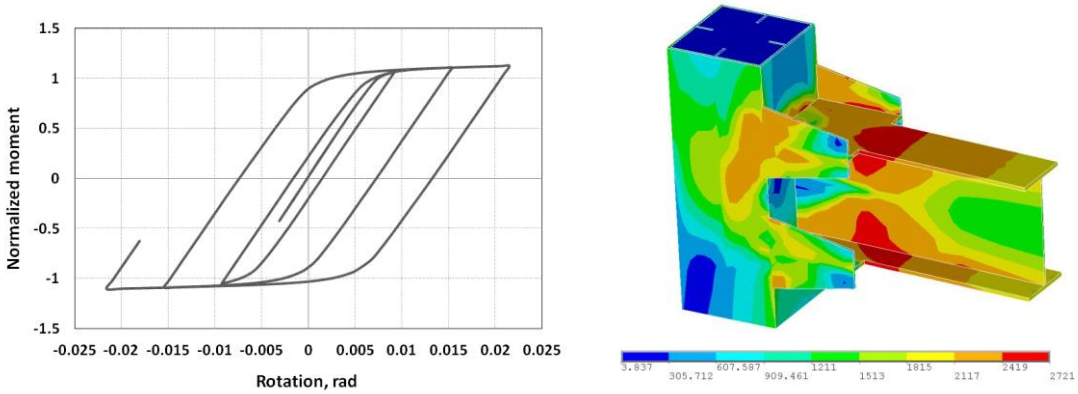

CI-2

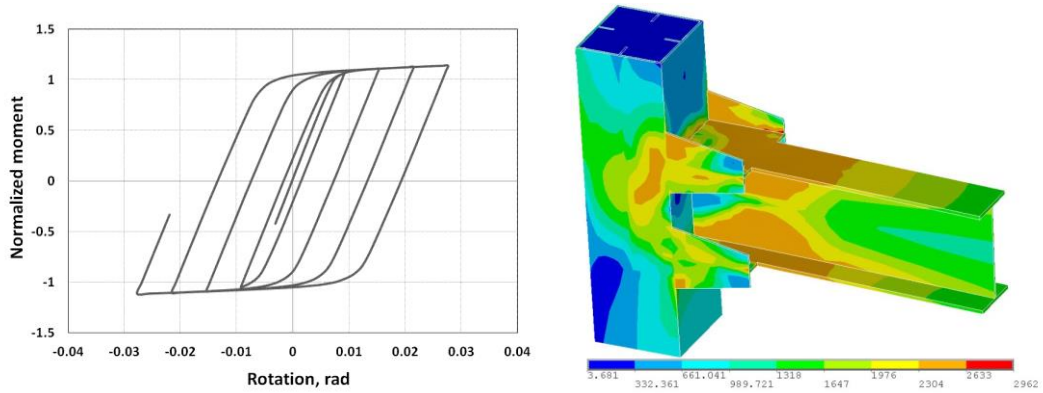

CI-3

Fig. 9 Hysteretic curves and stress distribution of the specimens in category I

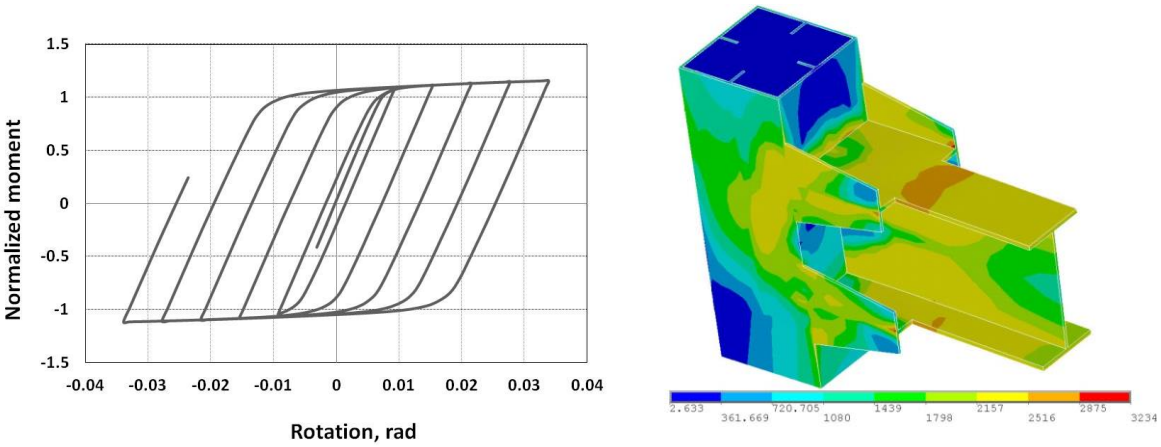

CI-4

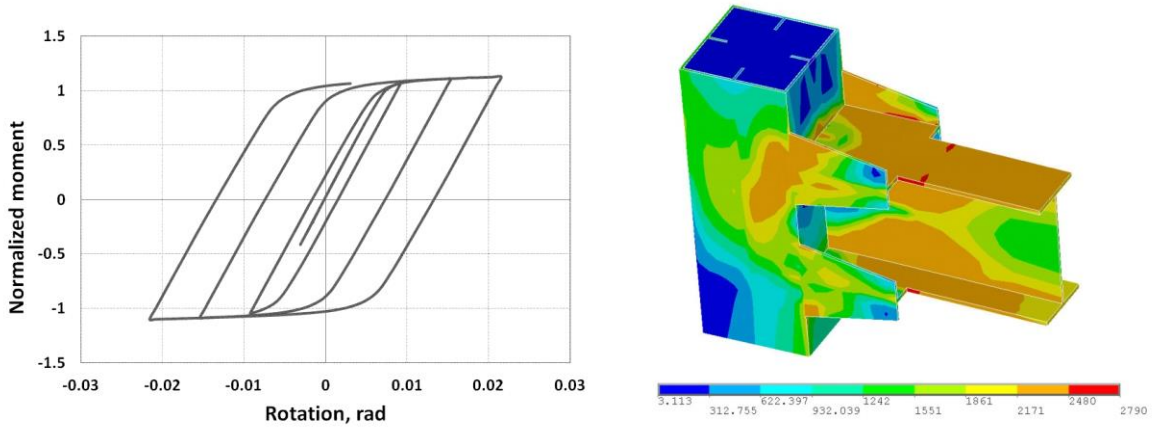

CI-5

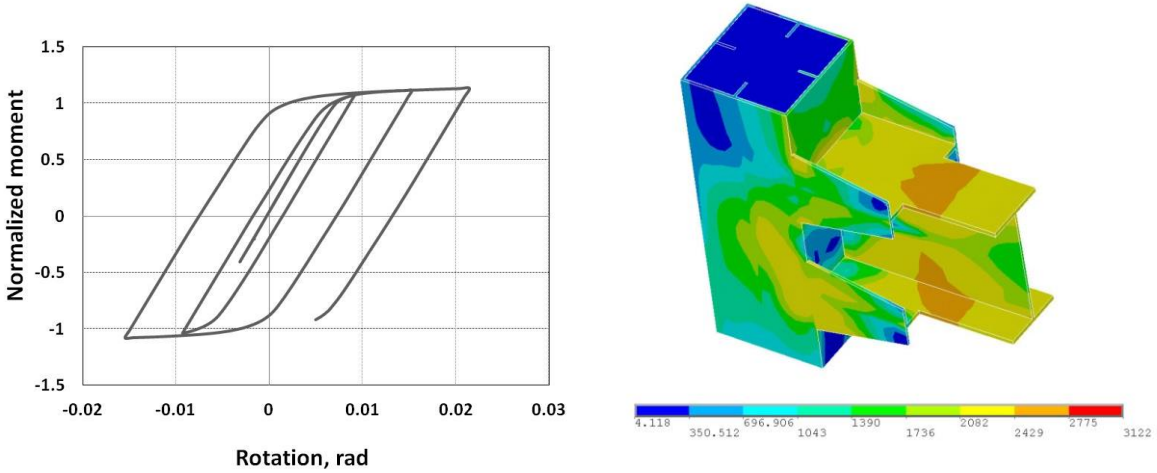

CI-6

Fig. 9 Continued

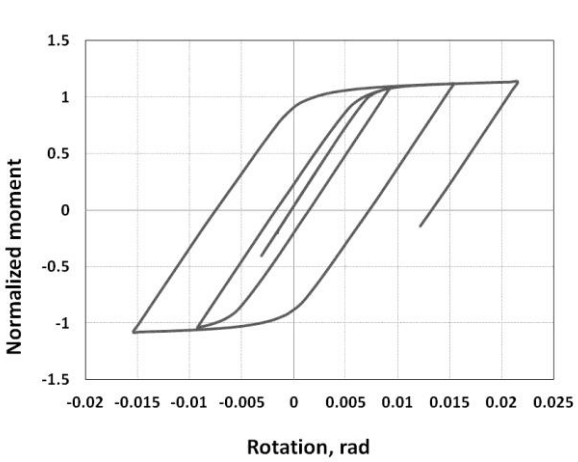

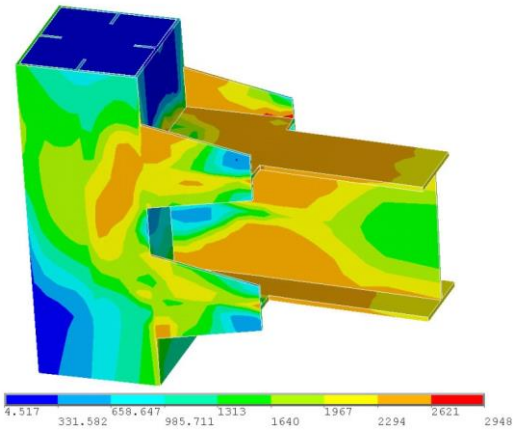

CI-7

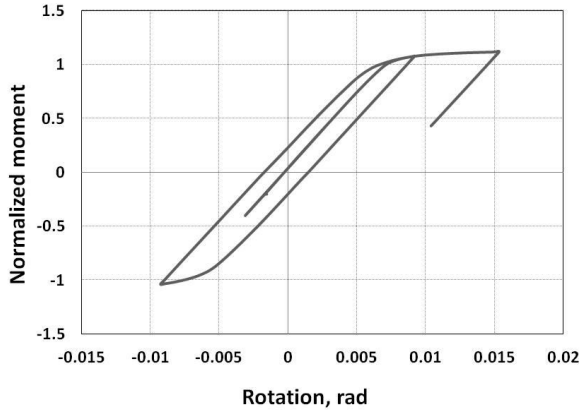

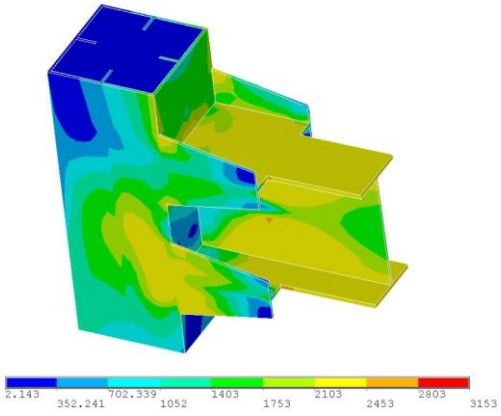

CI-8

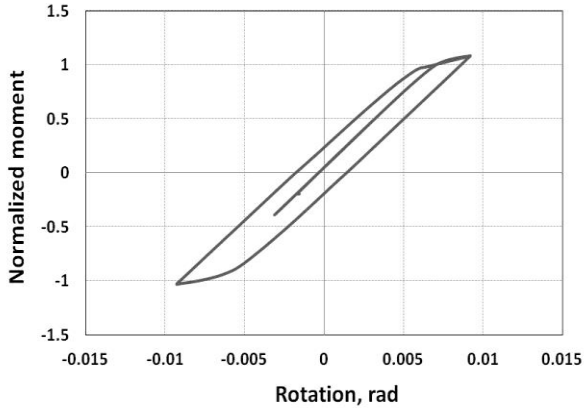

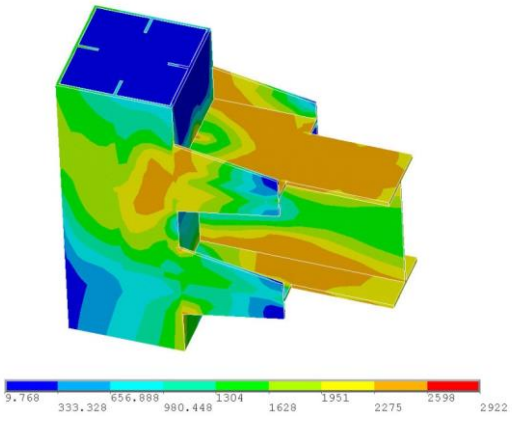

CI-9

Fig. 9 Continued

the column axial load. However, there is a threshold after which the rotation and energy dissipation capacity of the specimens significantly reduce. For the specimen considered in the current study, the optimal behaviour was observed in specimen CI-4 with a column axial load to ultimate strength ratio of 21%. However, the axial load on the column has a negligible effect on the lateral strength of the specimens.

4.2 Category II: Beam lateral support

The lateral support of the beam in a CFT connection can significantly affect its hysteretic behaviour. To investigate this, one specimen was analysed without providing any lateral support for the beam. The column axial load was considered to be about 21% of the ultimate strength of the column. All other conditions were the same as in previous specimens. As shown in Fig. 10, lack of the lateral support in a beam resulted in a lateral-torsional buckling failure at the sixth cycle. Compared to specimen CI-4, the ductility and energy dissipation capacity of the specimen CII-1 decreased significantly. Thus, restraining the lateral displacement of the beam can improve the seismic behaviour of a CFT connection. This condition is typically met in real three dimensional structures due to the existence of a floor deck.

4.3 Category III: Shape and arrangement of connection stiffeners

The effect of shape and arrangement of stiffeners in the hysteretic performance of a CFT connection were also investigated in the current study. Towards this end and to evaluate the effectiveness of other types of stiffeners compared to *T*-stiffener, seven specimens were considered. A summary of all specimens are provided in Table 5. These specimens were with

Table 4 Details of specimen in category II

Specimen Designation	No. of T-stiffeners	No. of Shear stiffeners	Ratio of column axial load to ultimate strength (%)
CII-1	4	4	21

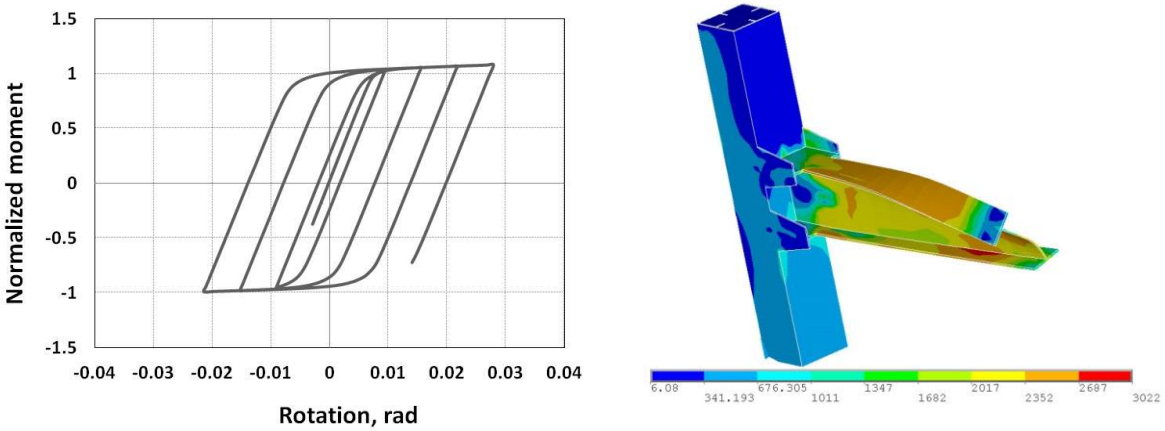

Fig. 10 Hysteretic curve and stress distribution at the last step of loading of specimen CII-1

doubler plate at column (CIII-1), top and bottom flange stiffeners (CIII-2, and CIII-3), horizontal stiffener only (CIII-4, and CIII-5), vertical stiffener only (CIII-6, and CIII-7), or without any stiffener (CIII-8). As with the previous specimens, four shear stiffeners were used to enhance the contact between concrete infill. In addition to using different stiffeners, two column axial loads ratio, 21% and 14%, were also implemented to account for the effect of axial loads. Also, a full lateral support was provided for the beams in all specimens.

Fig. 11 indicates the hysteretic curves and stress distribution in the last step of loading the specimens in category III. The analysis results outlined that the specimen behaved almost elastically and failed at the beginning of the second cycle. This was considered to be mainly due to the stress concentration at column tube attributed to the bending about the minor axes of the tube wall. As a result, the ultimate strength and rotation capacity of the specimens decreased substantially, compared to the specimens with T-stiffeners. This elaborates the vital role of the type of stiffener in CFT connections. Based on these results, application of T-stiffeners in CFT connections of real structures is more promising and beneficial.

Table 5 Details of specimens in category III

Specimen Designation	Stiffener Type	No. of Shear stiffeners	Ratio of column axial load to ultimate strength (%)
CIII-1	doubler plate stiffener	4	21
CIII-2	Top and bottom flange stiffeners	4	21
CIII-3	Top and bottom flange stiffeners	4	14
CIII-4	Horizontal stiffener only	4	21
CIII-5	Horizontal stiffener only	4	14
CIII-6	Vertical Stiffener only	4	21
CIII-7	Vertical Stiffener only	4	14
CIII-8	-	4	21

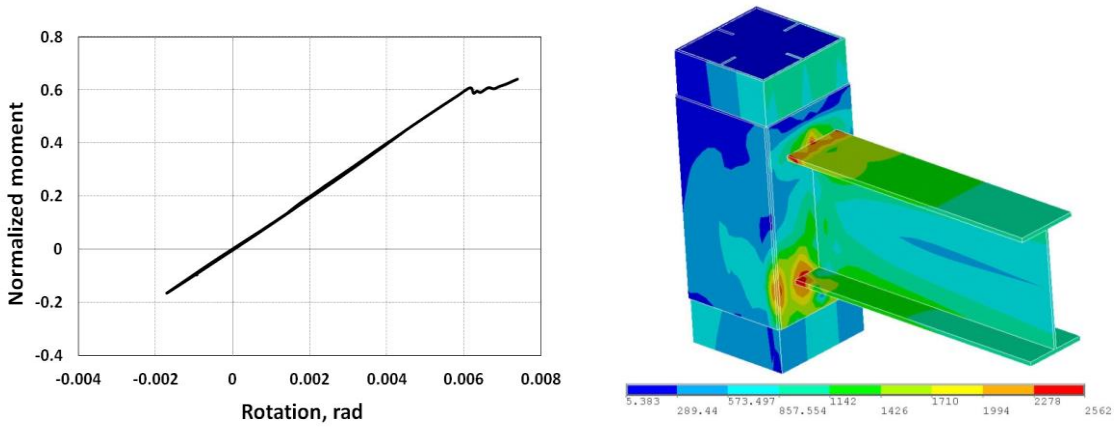

CIII-1

Fig. 11 Hysteretic curves and stress distribution of specimens in category III

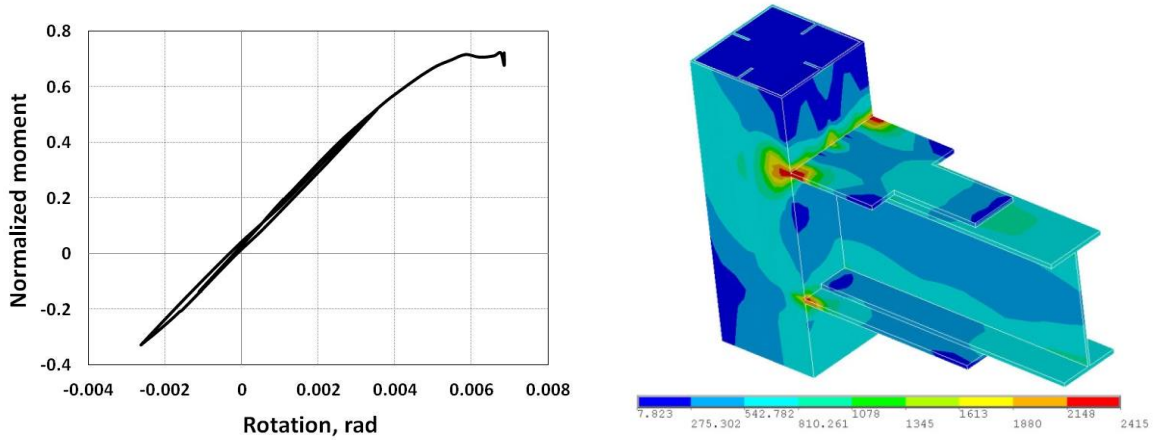

CIII-2

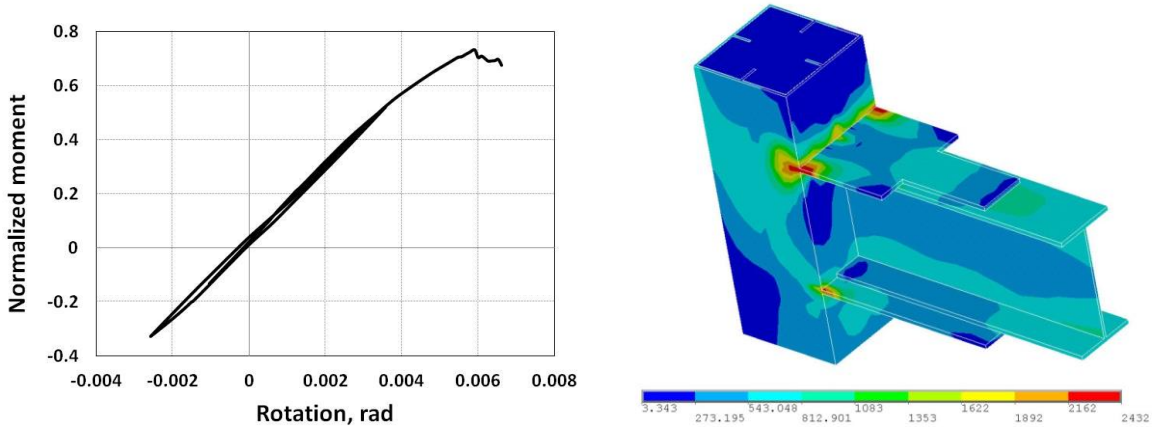

CIII-3

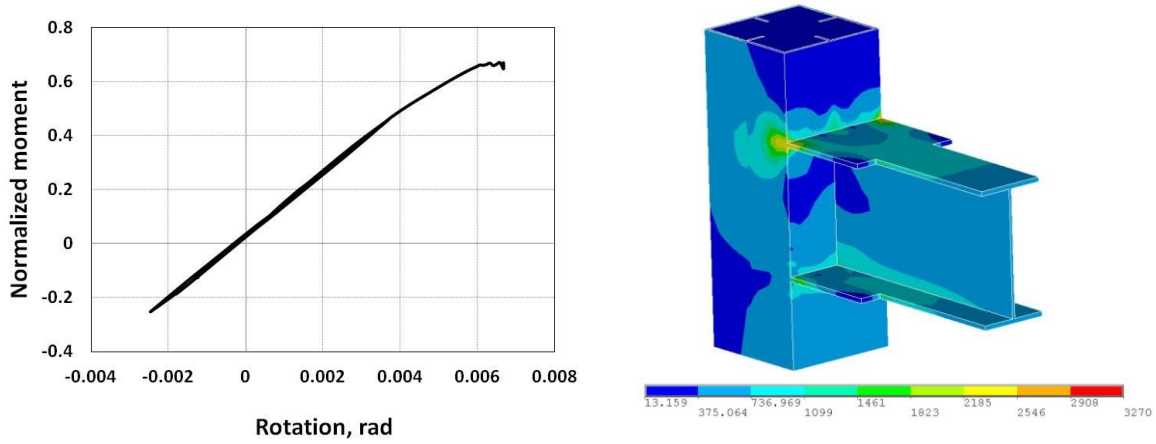

CIII-4

Fig. 11 Continued

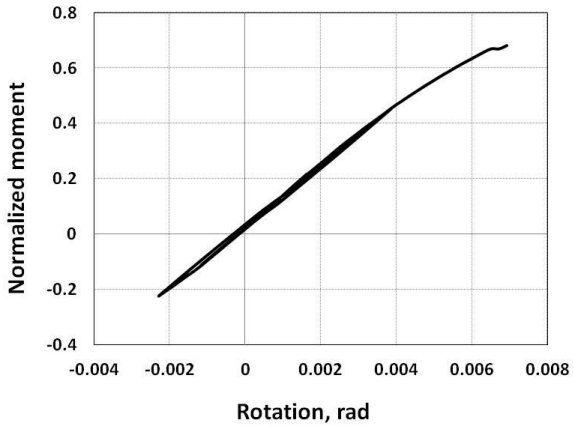

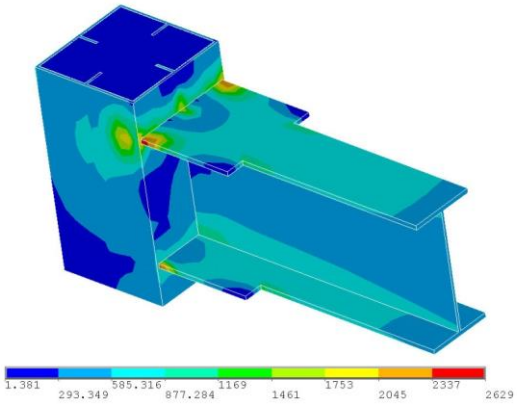

CIII-5

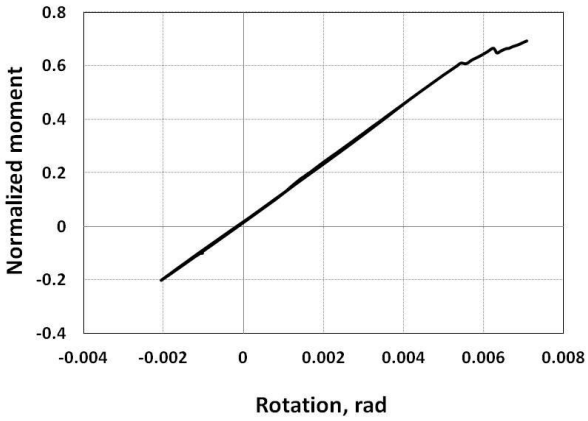

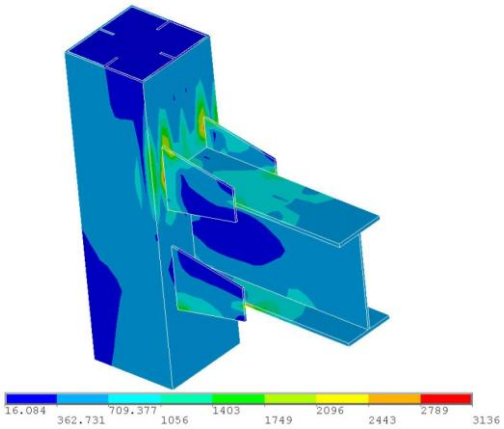

CIII-6

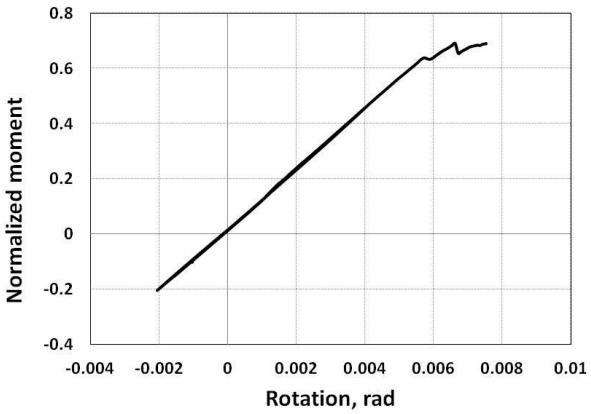

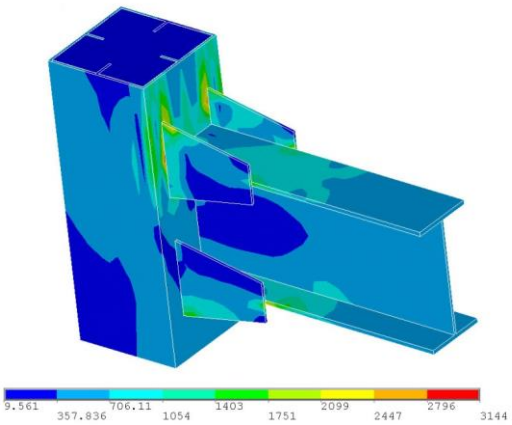

CIII-7

Fig. 11 Continued

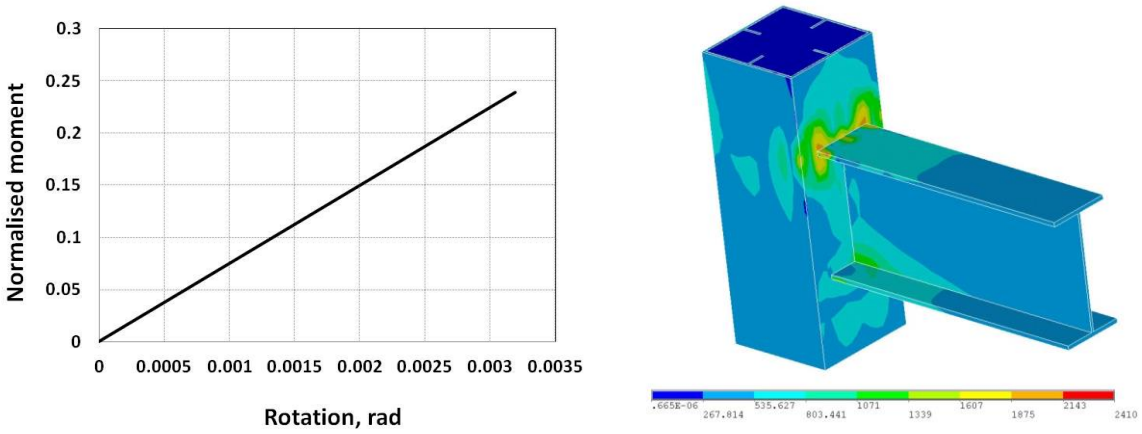

CIII-8

Fig. 11 Continued

Table 6 Details of specimens in category IV

Specimen Designation	No. of T-stiffeners	No. of Shear stiffeners	Ratio of column axial load to ultimate strength (%)
CIV-1	6	4	21
CIV-2	6	4	14

4.4 Category IV: Number of T-stiffeners

Amongst the important factors affected the behaviour of a CFT connection is the ratio of total strength of the *T*-stiffeners to the connected beam. To scrutinise the influence of this factor, two specimens were connected using six *T*-stiffeners. Table 6 provides the details of these two specimens. The lateral displacement of the beam was also fully prevented and four shear stiffeners were used with two different axial loads on the column.

The outcomes of the FE analyses of the specimens with six *T*-stiffeners are shown in Fig. 12. Compared to the specimen CI-4, the FE results of the specimen CIV-1 showed that increasing the strength of stiffeners has a negligible effect on the hysteretic behaviour of the CFT connections with an optimal column axial load. However, increasing the ratio of the total strength of *T*-stiffeners to the beam can significantly improve the hysteretic performance of the CFT connections with low column axial load. This conclusion can be observed from the FE results of the specimen CIV-2 compared to CI-3.

4.5 Category V: Number of shear stiffeners

The last parameter investigated during this study was the number of shear stiffeners inside the steel tube column. In practical construction, the shear stiffeners are used to increase the bond between concrete and steel in a CFT column. To evaluate the effect of shear stiffener on the cyclic behaviour of a CFT connection, the number of shear stiffeners was doubled in two specimens. Another specimen was also modelled without shear stiffeners. Table 7 summarizes a description of

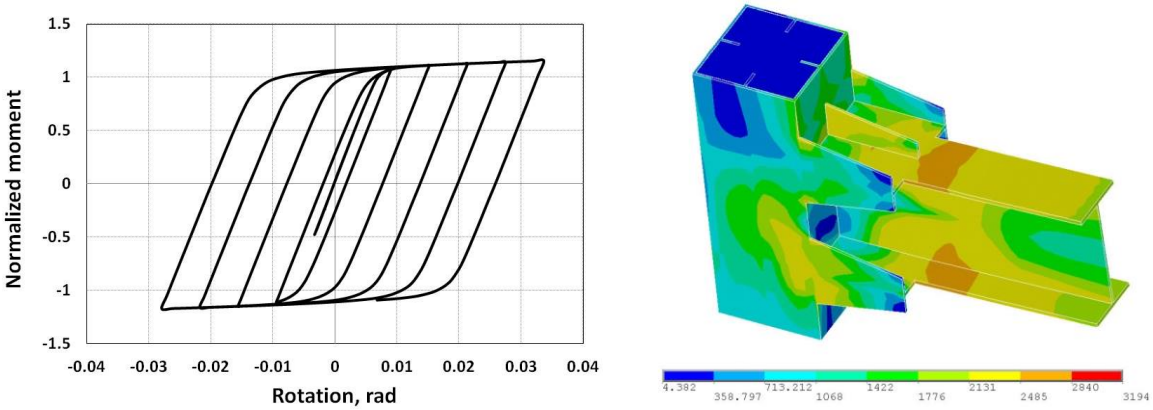

CIV-1

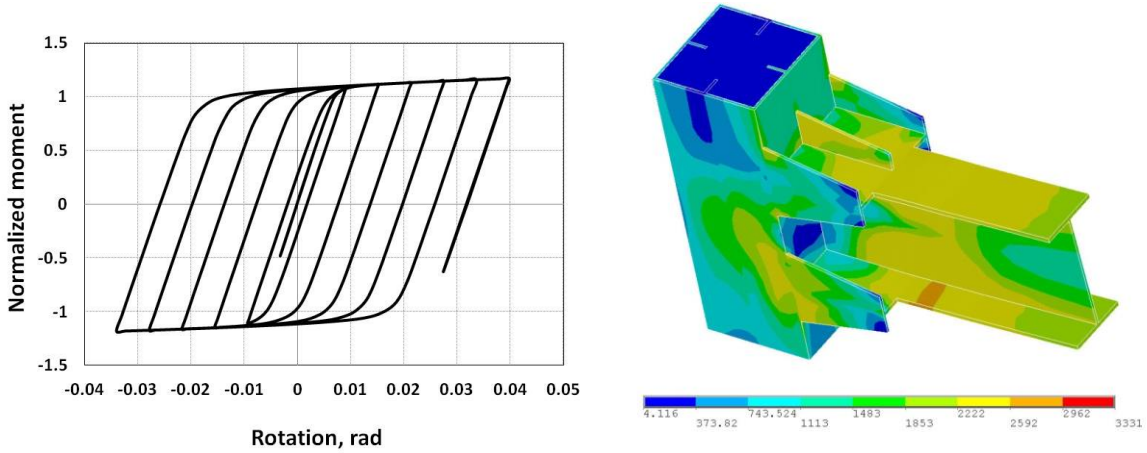

CIV-2

Fig. 12 Hysteretic curves and stress distribution of specimens in category IV

Table 7 Details of specimens in category V

Specimen Designation	No. of T-stiffeners	No. of Shear stiffeners	Ratio of column axial load to ultimate strength (%)
CV-1	4	8	23
CV-2	4	8	17
CV-3	4	0	17

these specimens. While the dimensions and number of the *T*-stiffeners and shear stiffeners were similar in all specimens, three different column axial loads were used in this category.

The hysteretic curves and distribution of stresses obtained at the last step of loading of the specimens are indicated in Fig. 13. Compared to the specimens with four shear stiffeners, the specimens with eight shear stiffeners could sustain more loading cycles and resulted in a significant increase in the energy dissipation capacity. In contrast, the specimen CV-4, which was without any shear stiffeners inside the steel tube, dissipated much less energy compared to

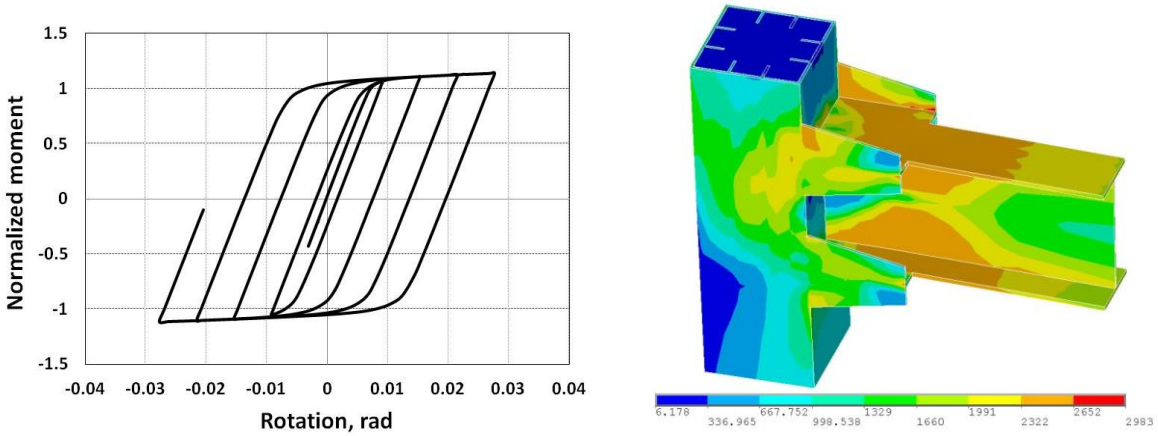

CV-1

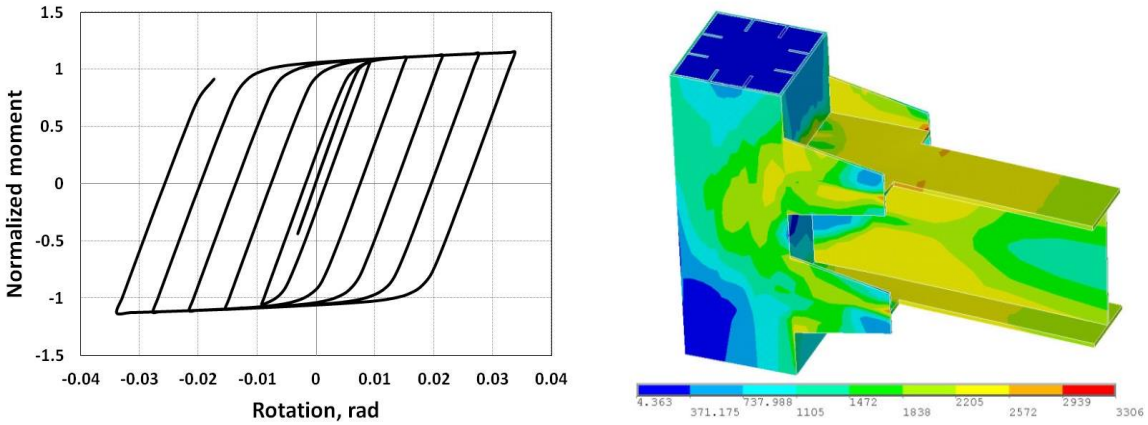

CV-2

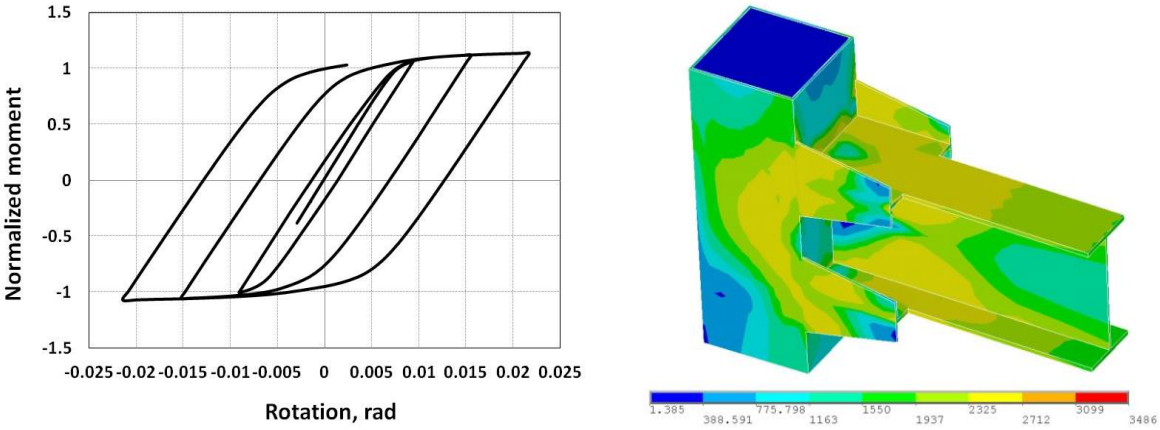

CV-3

Fig. 13 Hysteretic curves and stress distribution of specimens in category V

Table 8 Comparison of moment capacity, rotation capacity, and the cumulative dissipated energy for all specimens

Specimen Designation	Moment Capacity (kN.m)	Rotation Capacity (rad)	Cumulative energy dissipation (kN.m)
CI-1	1571	0.0215	74.8
CI-2	1562	0.0215	111.6
CI-3	1584	0.0276	216.1
CI-4	1603	0.0338	357.8
CI-5	1571	0.0215	123.7
CI-6	1575	0.0215	77.5
CI-7	1577	0.0215	71.9
CI-8	1561	0.0153	21.1
CI-9	1507	0.0092	12.8
CII-1	1496	0.0278	159
CIII-1	892	0.0074	0
CIII-2	1005	0.0068	0
CIII-3	1018	0.0066	0
CIII-4	929	0.0067	0
CIII-5	947	0.0069	0
CIII-6	964	0.0071	0
CIII-7	958	0.0075	0
CIII-8	332	0.0032	0
CIV-1	1602	0.0336	321.3
CIV-2	1624	0.0398	467.1
CV-1	1582	0.0276	221.5
CV-2	1596	0.0338	370
CV-3	1575	0.0217	114.2

specimen CV-3. As anticipated, increasing the number of shear stiffeners inside the steel tube can be considered as an effective factor in improving the cyclic behaviour of the CFT connection.

5. Discussion of the FE results

The results obtained from the nonlinear FE analysis of the developed models concluded the major contribution of the selected parameters in hysteretic performance of the CFT connections. Failure of each specimen was considered at a point after which the load was dropped by 20% of its ultimate capacity. A numerical comparison of moment capacity, rotation capacity, and the cumulative dissipated energy for all specimens is provided in Table 8. The area enclosed by each loading cycle is considered as the energy dissipated on that particular cycle. The cumulative energy dissipation is calculated by accumulating the energy dissipated in consecutive loops throughout the loading history. It should be noted that due to the symmetric geometry of the connection, the cyclic response of the specimens were identical in push and pull directions except for category III where the specimens failed in the elastic regions.

Considering the column axial load, the optimum hysteretic behaviour was observed in specimen CI-4 where the ratio of column axial load was about 21% of the column strength. This can be due to the interaction of moment and axial load in the column. Compared to other specimens, the specimens in category III indicated a considerable decrease in the moment and rotation capacity without any energy absorption due to the elastic behaviour of the specimens. This was particularly attributed to the use of stiffeners of a different shape than *T*-stiffeners. A close investigation of the FE results showed the stress concentration at the wall of the steel tube in this category lead to an early failure of the connection.

Also, the lateral support conditions for beam can noticeably affect the cyclic performance of the CFT connection. Specimen CII-1 was similar to specimen CI-4 except for providing the lateral support for a beam in the latter. However, the energy dissipation of specimen CI-4 was almost 2.25 times larger than specimen CII-1. In addition, the moment and rotation capacity of the former was reduced by 7% and 22%.

The specimen CIV-2 was comparable with specimen CI-3 in terms of column axial load. Increasing the number of T-stiffeners in the former resulted in a considerable increment in the dissipated energy, strength, and rotation capacity. However, the cyclic performance of specimens CIV-1 and CI-4 were almost identical.

Increasing the number of shear stiffeners could also significantly improve the cyclic behaviour of CFT specimens. The dissipated energy of specimens CV-1 and CV-2 was significantly larger than their corresponding specimens with four shear stiffeners (CI-5 and CI-3, respectively). In addition, the energy dissipation of specimen CV-3, which was without shear stiffeners, was decreased by 69% compared to specimen CV-2.

6. Conclusions

This paper reports on the results of a parametric investigation on the hysteretic behaviour of composite CFT column to I-beam connections. Following the verification of the nonlinear modelling against the existing experimental data, a total of twenty-three CFT connections were modelled to evaluate the effect of different parameters including column axial load, beam lateral support, type of stiffeners, number of T-stiffeners, and number of shear stiffeners. Based on the results obtained, the following conclusions were drawn:

• Increasing the column axial load can remarkably improve the ultimate rotation (displacement) and dissipated energy of a CFT connection under cyclic loading. However, there is a threshold after which the rotation and energy dissipation capacity reduce significantly. For the specimen analysed in the current study, the optimum behaviour was observed at the ratio of column axial load to ultimate strength of 21% (Specimen CI-4). It should be noted that the column axial load has a negligible effect on the ultimate moment capacity of a CFT connection under cyclic loading.

• Lateral supporting of the beam in a CFT connection can noticeably improve the hysteretic responses of a CFT connection. For the case-study analysed in this investigation, the ultimate rotation and energy dissipation capacity of the specimen without beam lateral support, CII-1, were reduced by 22% and 125%, respectively compared to their counterparts measured from specimen CI-4. The lateral support for beam in CFT structures is generally provided when the beam is supported by floor slabs and/or joists in real construction.

• Compared to the specimens with T-stiffeners, the specimens in category III indicated a considerable decrease in the moment and rotation capacity without any energy absorption due to

the elastic behaviour of the specimens. Failures of the specimens in category III were mainly attributed to the high stress concentration as the tube wall. This outlined the efficiency of the T-stiffeners in transferring the beam forces to the column. Therefore, this type of stiffener is highly recommended in real CFT construction.

• Increasing the number of T-stiffeners may not affect the hysteretic behaviour of a CFT connection at its optimal column axial load. However, it can significantly increase the ultimate rotation and energy dissipation capacity of a CFT connection at column axial loads lower that the optimum. This conclusion can be clearly observed comparing the analysis results of the specimens CIV-2 and CI-3. Taking into consideration that the axial load on column can change during a seismic loading and considering the conditions of real construction, application of higher number of T-stiffeners is recommended in CFT connections.

• Shear stiffeners can directly influence the hysteretic behaviour of a CFT connection under cyclic loading. For the case-study specimen of this study, the energy dissipation of the specimen without shear stiffener was 69% lower than its counterpart with eight shear stiffeners.

Overall, the lateral support, T-stiffeners, and shear stiffeners have a positive effect on the hysteretic performance of a CFT column to steel beam connection. Regarding the column axial load, it is recommended that the CFT connections are designed with a low ratio of column axial load to ultimate strength. However, more studies should be conducted to further investigate the effect of column axial load in CFT connections.

References

Abedi, K., Ferdousi, A. and Afshin, H. (2008), "A novel steel section for concrete-filled tubular columns", *Thin Wall. Struct.*, **46**(3), 310-319.

ANSYS Manual (2005), 9 Edition, Canonsburg, PA 15317, USA.

Dalalbashi, A., Eslami, A. and Ronagh, H.R. (2012), "Plastic hinge relocation in RC joints as an alternative method of retrofitting using FRP", *Compos. Struct.*, **94**(8), 2433-2439.

Dalalbashi, A., Eslami, A. and Ronagh, H.R. (2013), "Numerical investigation on the hysteretic behavior of RC joints retrofitted with different CFRP configurations", *J. Compos. Construct.*, **17**(3), 371-382.

Elremaily, A. and Azizinamini, A. (2001), "Experimental behavior of steel beam to CFT column connections", *J. Construct. Steel Res.*, **57**(10), 1099-1119.

Eslami, A., Dalalbashi, A. and Ronagh, H.R. (2013), "On the effect of plastic hinge relocation in RC buildings using CFRP", *Compos. Part B: Eng.*, **52**, 350-361.

Eslami, A. and Ronagh, H.R. (2013), "Effect of FRP wrapping in seismic performance of RC buildings with and without special detailing-A case study", *Compos. Part B: Eng.*, **45**(1), 1265-1274.

Eslami, A., Ronagh, H.R., Mahini, S.S. and Morshed, R. (2012), "Experimental investigation and nonlinear FE analysis of historical masonry buildings-A case study", *Construct. Build. Mater.*, **35**, 251-260.

Gardner, A.P. and Goldsworthy, H.M. (2005), "Experimental investigation of the stiffness of critical components in a moment-resisting composite connection", *J. Construct. Steel Res.*, **61**(5), 709-726.

Ghobadi, M.S., Ghassemieh, M., Mazroi, A. and Abolmaali, A. (2009), "Seismic performance of ductile welded connections using T-stiffener", *J. Construct. Steel Res.*, **65**(4), 766-775.

Ghobadi, M.S., Mazroi, A. and Ghassemieh, M. (2009), "Cyclic response characteristics of retrofitted moment resisting connections", *J. Construct. Steel Res.*, **65**(3), 586-598.

Han, L.H., Wang, W.D. and Tao, Z. (2011), "Performance of circular CFST column to steel beam frames under lateral cyclic loading", *J. Construct. Steel Res.*, **67**(5), 876-890.

Hassan, M.M., Ramadan, H.M., Naeem, M. and Mourad, S.A. (2014), "Behaviour of gusset plate-T0-CCFT connections with different configurations", *Steel Compos. Struct.*, **17**(5), 735-751.

Kachlakev, D., Miller, T., Yim, S., Chansawat, K. and Potisuk, T. (2001), "Finite element modeling of reinforced concrete structures strengthened with FRP laminates", SPR 316. Oregon Department of Transportation Research Group and Federal Highway Administration.

Kang, C.H., Shin, K.J., Oh, Y.S. and Moon, T.S. (2001), "Hysteresis behavior of CFT column to H-beam connections with external T-stiffeners and penetrated elements", *Eng. Struct.*, **23**(9), 1194-1201.

Kang, L., Leon, R.T. and Lu, X. (2015), "Shear strength analyses of internal diaphragm connections to CFT columns", *Steel Compos. Struct.*, **18**(5), 1083-1101.

Kiamanesh, R., Abolmaali, A. and Ghassemieh, M. (2010), "The effect of stiffeners on the strain patterns of the welded connection zone", *J. Construct. Steel Res.*, **66**(1), 19-27.

Lee, C.H. Kim, J.W. and Song, J.G. (2008), "Punching shear strength and post-punching behavior of CFT column to RC flat plate connections", *J. Construct. Steel Res.*, **64**(4), 418-428.

Liu, J., Zhou, X. and Zhang, S. (2008), "Seismic behaviour of square CFT beam-columns under biaxial bending moment", *J. Construct. Steel Res.*, **64**(12), 1473-1482.

Mirghaderi, S.R., Torabian, S. and Keshavarzi, F. (2010), "I-beam to box-column connection by a vertical plate passing through the column", *Eng. Struct.*, **32**(8), 2034-2048.

Probst, A., Kang, T., Ramseyer, C. and Kim, U. (2010), "Composite flexural behavior of full-scale concrete-filled tubes without axial loads", *J. Struct. Eng.*, **136**(11), 1401-1412.

Rashid, Y.R. (1968), "Ultimate strength analysis of prestressed concrete pressure vessels", *Nucl. Eng. Des.*, **7**(4), 334-344.

Razzaghi, M.S., Esfandyary, R. and Nateghi, A.F. (2014), "The effects of internal and external stiffeners on hysteretic behavior of steel beam to CFT column connections", *IJE Tran. A: Basic.*, **27**(7), 1005-1014.

Ronagh, H.R. and Baji, H. (2014), "On the FE modeling of FRP-retrofitted beam–column subassemblies", *Int. J. Concrete Struct. Mater.*, **8**(2), 141-155.

Schneider, S.P. and Alostaz, Y.M. (1998), "Experimental Behavior of Connections to Concrete-filled Steel Tubes", *J. Construct. Steel Res.*, **45**(3), 321-352.

Sheet, I. S., Gunasekaran, U., and Macrae, G. A. (2013), "Experimental investigation of CFT column to steel beam connections under cyclic loading", *J. Construct. Steel Res.*, **86**, 167-182.

Shin, K.J., Kim, Y.J. and Oh, Y.S. (2008), "Seismic behaviour of composite concrete-filled tube column-to-beam moment connections", *J. Construct. Steel Res.*, **64**(1), 118-127.

Shin, K.J., Kim, Y.J., Oh, Y.S. and Moon, T.S. (2004), "Behavior of welded CFT column to H-beam connections with external stiffeners", *Eng. Struct.*, **26**(13), 1877-1887.

Willam, K.J. and Warnke, E. . (1975), "Constitutive model for the triaxial behaviour of concrete", *Proceedings of International Association for Bridge and Structural Engineering*, Bergamo, Italy.

Wu, L.Y., Chung, L.L., Tsai, S.F., Lu, C.F. and Huang, G.L. (2007), "Seismic behavior of bidirectional bolted connections for CFT columns and H-beams", *Eng. Struct.*, **29**(3), 395-407.

Yuan, H., Dang, J. and Aoki, T. (2014), "Behavior of partially concrete-filled steel tube bridge piers under bi-directional seismic excitations", *J. Construct. Steel Res.*, **93**, 44-54.

Zhang, D., Gao, S. and Gong, J. (2012), "Seismic behaviour of steel beam to circular CFST column assemblies with external diaphragms", *J. Construct. Steel Res.*, **76**, 155-166.

Zhao, X.L., Tong, L.W. and Wang, X.Y. (2010), "CFDST stub columns subjected to large deformation axial loading", *Eng. Struct.*, **32**(3)**,** 692-703.

CC